Available online at www.sciencedirect.com

SCIENCE DIRECT®

Catalysis Today 93–95 (2004) 553–560

CATALYSIS TODAY

www.elsevier.com/locate/cattod

Development of nickel catalyst supported on MgO–TiO_2 composite oxide for DIR-MCFC

Jae-Suk Choi [a], Heock-Hoi Kwon [b], Tae-Hoon Lim [c], Seong-Ahn Hong [c], Ho-In Lee [a,*]

[a] School of Chemical Engineering and Research Center for Energy Conversion and Storage, Seoul National University, Seoul 151-744, South Korea
[b] Department of Chemical and Environmental Engineering, Soongsil University, Seoul 156-743, South Korea
[c] Fuel Cell Research Center, Korea Institute of Science and Technology, Seoul 136-791, South Korea

---

Abstract

As an effort to synthesize supported Ni reforming catalysts resistant to Li poisoning, which is essential in commercializing the direct internal reforming molten carbonate fuel cells (DIR-MCFC), a series of Ni catalysts supported on MgO–TiO_2 composite oxides with varying ratio of Mg to Ti were prepared. Under the Li-free condition, the supported Ni reforming catalysts were active regardless of the ratio of Mg to Ti; however, when Li was introduced to the catalysts, the catalysts lost their activities with different degrees. Temperature-programmed reduction (TPR) and X-ray diffraction (XRD) results indicated that the addition of relatively small fraction of TiO_2 into the NiO/MgO catalyst system was effective in obstructing the formation of $Ni_xMg_{1-x}O$ solid solution and in increasing resistance to Li poisoning. The Ni catalysts supported on the composite oxides with Mg/Ti ratios of 2–7 turned out to be far more resistant to Li poisoning, showing approximately 60% of their original activities even under severe lithium carbonate condition, than the ones with other Mg/Ti ratios.

Keywords: DIR-MCFC; Nickel catalyst; MgO–TiO_2 composite oxide; Metal–support interaction

---

1. Introduction

As a novel route to produce cleaner and more economical electric power, many topics in molten carbonate fuel cell (MCFC) have been studied extensively for decades. By positioning the reforming catalyst in anode chamber, the direct internal reforming MCFC (DIR-MCFC) takes advantage of thermal benefit by using exothermic heat of electrochemical reaction on anode for endothermic reforming reaction as well as increased conversion of methane due to in situ consumption of hydrogen. However, there are fundamental problems to solve prior to practical applications such as deterioration of reforming catalyst by alkali carbonates contained in the electrolyte matrix [1].

Since alkali carbonates were known to deactivate the reforming catalyst, many efforts have been made to deal with this deactivation problem [2–4]. Resultantly, there were progresses in elucidating transport mechanism of alkali species from the electrolyte to catalyst [5,6] and in understanding the role of alkalis (Li, Na and K) in physicochemical changes of catalysts supported on various metal oxides [4,7].

For deactivation processes, covering and faceting, sintering of support and active nickel, and blocking of pore structure were suggested [3,7]. Among these processes, sintering of the supported nickel was commonly regarded as the major reason for catalyst deactivation. Matsumura and Hirai [7] maintained that alkali deteriorated the stability of support severely. Among the alkali species, lithium seemed to be the most notorious in poisoning the Ni reforming catalyst. Moon et al. [8–10] reported the deactivation of the Ni/MgO catalyst operated in DIR-MCFC single cell for 72 h. They suggested that lithium was the most harmful among alkalis evaluated and that deactivation of the catalyst was mainly due to the formation of solid solution, which resulted in nickel sintering. Their results are somewhat consistent with those of Arena et al. [11–13] in which the morphology and dispersion of Ni/MgO catalysts were greatly affected by Li added by impregnation during catalyst preparation, via the change of NiO–MgO interaction. In addition, Antolini [14] reported that Li/Ni/MgO system changed to ternary $Li_yNi_xMg_{1-y-x}O$ solid solution by air calcination.

The support materials employed in published papers for the Ni reforming catalysts include magnesia, alumina and mixtures of magnesia and alumina having the spinel structure. Understanding the effects of alkalis on each support

---

* Corresponding author. Tel.: +82 2 880 7072; fax: +82 2 888 1604.
E-mail address: hilee@snu.ac.kr (H.-I. Lee).

0920-5861/$ – see front matter © 2004 Elsevier B.V. All rights reserved.
doi:10.1016/j.cattod.2004.06.004

material and supported Ni regarding solid-state chemistry and strength of metal-to-support interaction must be essential for further development of the reforming catalysts resistant to alkalis. Fundamental studies to understand how to manipulate interactions and chemistries among Li, Ni, and support materials by changing compositions and/or adding other metal oxides must further stimulate the development of the DIR-MCFC.

The NiO–MgO system is famous for making ideal solid solution over the whole atomic fraction ranges. This implies that supported nickel catalyst on MgO has strong metal–support interaction, which made this catalyst attractive for the versatile applications including methane partial oxidation [15,16]. Titanium oxide is also known to have strong interaction with Ni and has been used as support for many reactions [17]. In order to develop a new support system for Ni loading that minimizes Li poisoning by altering the catalyst–support interaction, we introduced TiO_2 to MgO support and achieved substantial resistance to lithium poisoning as previous reported [18]. There are three different crystalline structures for the MgO–TiO_2 composite oxide system depending on the Mg/Ti ratio: karooite ($MgTi_2O_5$), geikielite ($MgTiO_3$), and qandilite (Mg_2TiO_4). Although the synthesis and characteristics of those composites were previously studied as a catalyst [19–21], no report was found concerning the application of the composites as a catalyst support.

In this paper, we prepared a series of nickel catalysts supported on MgO–TiO_2 composite oxides with varying Mg to Ti ratio, and evaluated their catalytic properties and resistances to Li poisoning. The prepared catalysts were characterized by TPR, XRD, and BET. Changes in interactions between metal and support by varying Mg to Ti ratio were discussed and correlated to the catalytic properties and resistances to Li poisoning.

2. Experimental

2.1. Preparation of the catalysts

Synthetic procedure for MgO–TiO_2 composite oxides as a support is as follows. Magnesium acetate and titanium tetraisopropoxide were dissolved in water and isopropyl alcohol, respectively. Corresponding precursor solution of magnesium was dropped to the solution of the titanium tetraisopropoxide until target Mg/Ti ratios were achieved, and then aged for 3 h. After drying at 80 °C, sticky gels were obtained. In order to remove the solvent completely, the gels were vacuumed at 50 °C for 24 h. Then, the evacuated composite oxides were grinded, heated up to 700 °C at 5 °C/min, and calcined at 700 °C for 12 h. Magnesium oxide support materials were catalyst was prepared by calcining magnesium hydroxide at 700 °C for 12 h. The titanium oxide employed was P25 (Degussa) and used as purchased. The samples were coded to M_xT where x means the molar ratio of Mg to Ti.

The active component, nickel, was loaded using the deposition–precipitation method following a reference article [15]. Nickel nitrate solution (0.22 M) was injected into a suspension of the support in 2 L deionized water. The injection was controlled by a micro syringe pump (Keun-A, KASP005) at 0.5 mL/min, and finished upon reaching the amount corresponding to 30 wt.% of nickel loading. The pH was controlled to be approximately 10 by simultaneous injection of 1.5 M ammonia solution. After precipitation precursors were washed with 2 L of demineralized water and dried at 50 °C under vacuum overnight. Then, the supported nickel catalysts were oxidized in liquid phase with NaOCl for 12 h at 80 °C [22]. The samples were filtered and washed using a large amount of deionized water and then dried under vacuum again. The catalyst supported on TiO_2 (P25) did not pass through liquid oxidation process. The precursors were calcined for 30 min at temperatures in the range of 300–700 °C.

2.2. Catalytic activity test and deactivation

The catalytic reactions were conducted in quartz tube reactor at 650 °C under atmospheric pressure, which is similar condition used actually in MCFC [23]. A thermowell equipped with a K-type thermocouple was placed in the center of catalyst bed. A controlled amount of CH_4 and H_2O with molar ratio of 1:2.5 was fed into the reactor by a mass flow controller and a micro syringe, respectively. The flow rate of methane was 20 sccm. For each run, 100 mg of catalyst was activated at 650 °C for 30 min in flowing H_2/N_2 mixture (30/30 v/v) prior to the reforming reaction. Gaseous effluents were passed through a trap maintained at 0 °C to remove the unreacted water and then analyzed by on-line gas chromatography (Donam) equipped with a TCD detector using Ar as carrier gas.

In order to study Li poisoning, stability tests were carried out. The lithium carbonate powder (99%, Avondale Laboratories) was mechanically mixed with the catalysts, and then the catalysts having Li_2CO_3 were treated in flowing hydrogen at 650 °C for 2 h. Amount of Li_2CO_3 used was expressed in wt.% based on the weight of Li-free catalysts and denoted to xL- as prefix in catalyst codes. For example, 30L-M_5T stands for the catalyst having Mg five times more than Ti in the support being mixed with 30 wt.% of Li_2CO_3.

2.3. Characterization

The powder X-ray diffraction (XRD) with a Mac Science M18XHF^{22}-SRA diffraction spectrometer using Cu Kα as a radiation source was used to determine the phases of the prepared samples. Temperature-programmed reduction (TPR) was performed by heating samples from room temperature to 900 °C at 10 °C/min in 10% H_2 in N_2 balance flowing at 33 cc/min. A cold ethanol trap maintained at −40 °C was placed to capture moisture before inlet of TCD cell in the TPR system.

Table 1
Nickel loadings on the Ni/MgO–TiO_2 composite oxides with varying Mg/Ti ratios analyzed by ICP

	1	2	3	4	5	6	7	8	9
Mg/Ti ratio	0.57	0.97	1.42	2.19	2.99	3.52	5.10	6.80	7.88
Ni loading (wt.%)	30.1	30.6	37.7	30.5	29.3	27.2	26.2	26.4	25.3
Code[a]	$M_{0.6}T$	M_1T	$M_{1.5}T$	$M_{2.2}T$	M_3T	$M_{3.5}T$	M_5T	M_7T	M_8T

[a] Each sample was coded to M_xT where x represented the molar ratio of Mg to Ti.

The BET surface areas were determined by N_2 adsorption by ASAP 2010 (Micromeritics). Each sample was pretreated at 150 °C under high vacuum prior to analysis.

3. Results

3.1. Preparation of nickel catalysts supported on MgO–TiO_2 composite oxides

Table 1 showed the Ni loading analyzed by induced coupled plasma (ICP) for the prepared catalyst samples. The samples were coded by the molar ratio of Mg to Ti as explained in Section 2. The Ni loadings were between 25 and 31% except the $M_{1.5}T$ sample.

3.2. Activities of Li-free catalysts and deactivated catalysts

The prepared samples were evaluated by the steam reforming reaction with methane and summarized in Table 2. The “30L” denotes the catalyst deactivated by lithium carbonate as described above. The activities of samples calcined at 700 °C for 30 min were also listed to investigate the effects of calcination temperature. The conversions of the uncalcined catalyst samples were around 65–80% with one exception. When the samples were calcined at 700 °C, the activities of all samples decreased. We believe it is due to nickel sintering by experiencing high temperature. After Li poisoning methane conversions of all samples decreased, although the decreased degrees were different for each sample. The catalyst samples having the Mg/Ti ratio of 2–7 sustained relatively high activities. For the “30L” catalyst samples calcined at 700 °C showed more activities than the uncalcined ones except for the samples rich in magnesia such as M_8T and MgO. Pure oxides, magnesia and titania, behaved differently from each other. The uncalcined Ni/TiO_2 catalyst lost all of its activity after Li poisoning, while the calcined one did not. For the Ni/MgO samples, Li poisoning made the samples almost inactive regardless of calcination.

3.3. BET surface area

The BET surface areas of the samples calcined at 300 °C and the deactivated ones with 30 wt.% Li_2CO_3, denoted by 30L, were shown in Table 3. For the Li-free catalysts, BET surface areas had a tendency to increase with Mg fraction increase in support with a few exceptions. After Li poisoning, the catalyst samples lost their surface areas drastically.

3.4. Temperature-programmed reduction (TPR)

The TPR spectra of nickel supported on TiO_2 and MgO were shown in Figs. 1 and 2, respectively. In Fig. 1, all of peaks seemed to be consisted of two peaks: (a) 300 and 306 °C, (b) 320 and 400 °C, (c) 390 and 470 °C, (d) 590 and 640 °C. The peaks of each sample shifted to higher temperatures as calcination temperature increased. In the case of the sample calcinations at 700 °C, there was no Ni reduction peak at ∼400 °C.

The patterns of Ni reduction for the NiO/MgO samples were entirely different from the ones for the NiO/TiO_2. The nickel on MgO revealed a single broad peak of reduction. The shape and position of peaks in the spectra for the samples of uncalcined and calcined below 500 °C or below changed insignificantly. For the samples calcined at 700 and 900 °C, reduction peaks of nickel disappeared and tended to shift to higher temperatures.

The TPR results of nickel supported on $M_{2.2}T$ were shown in Fig. 3. The peaks at ∼300 °C disappeared and the ones between 400 and 600 °C shifted to higher temperatures as calcination temperatures were increased. The reductive behavior of NiO/$M_{2.2}T$ was different from that of NiO/TiO_2.

Table 2
The activities of the prepared Ni reforming catalysts before and after Li poisoning

	TiO_2	$M_{0.6}T$	M_1T	$M_{1.5}T$	$M_{2.2}T$	M_3T	M_5T	M_7T	M_8T	MgO
Li free										
Uncalcined	67.3	86.3	55.3	66.2	83.6	78.9	79.3	80.2	79.3	64.9
Calcined at 700 °C	55.1	58.6	45.2	60.0	73.7	80.2	70.2	62.0	59.6	66.1
30L										
Uncalcined	0	11.4	6.4	1.4	43.4	44.2	32.2	33.9	7.4	0.9
Calcined at 700 °C	12.5	8.9	20.6	39.2	48.8	48.6	42.3	41.7	2.6	0

Table 3
The BET surface areas (m^2/g) of the prepared Ni reforming catalysts before and after Li poisoning

	$M_{0.6}T$	M_1T	$M_{1.5}T$	$M_{2.2}T$	M_3T	M_5T	M_7T	M_8T	MgO
Li free	89.1	66.9	70.6	107.1	96.4	150.9	180.3	196.2	115
30L	10.2	9.5	12.7	22.2	20.9	26.1	38.9	37.3	16.2

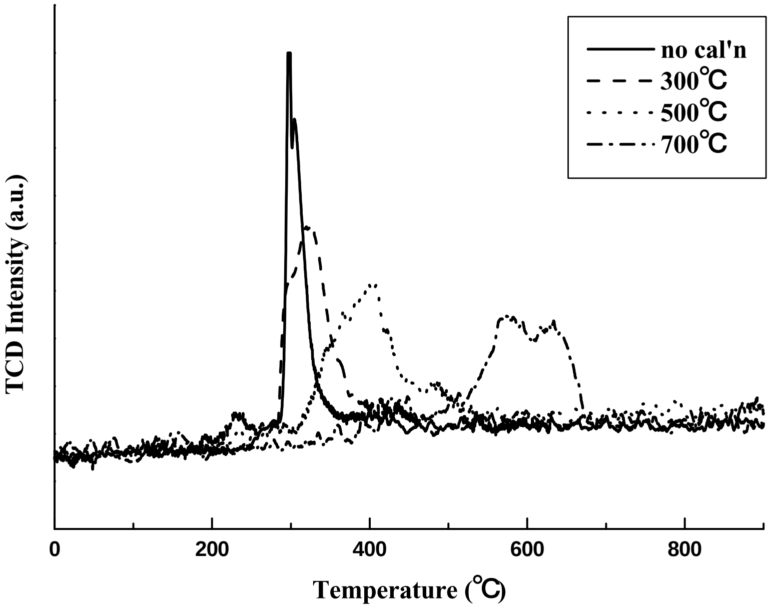

Fig. 1. The TPR spectra of NiO/TiO$_2$ calcined at various temperatures.

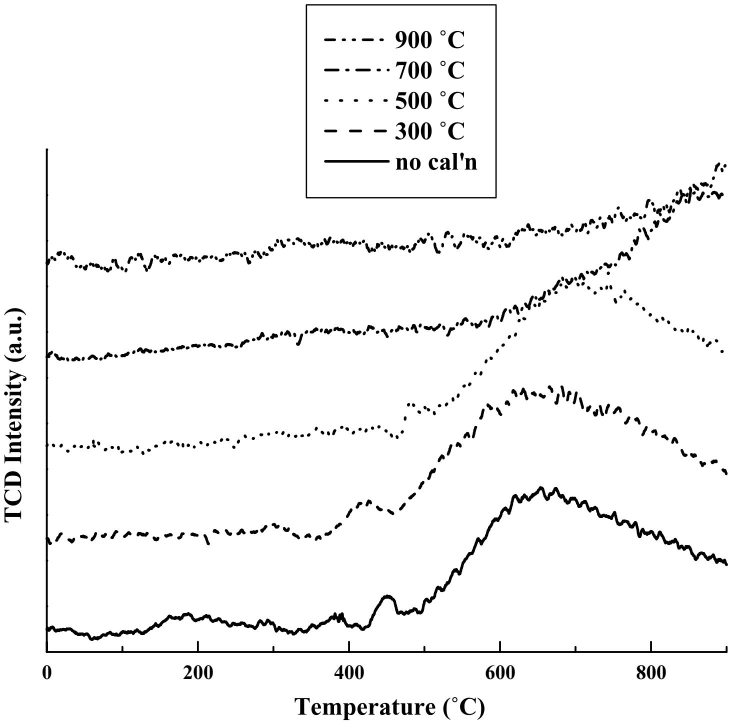

Fig. 2. The TPR spectra of NiO/MgO calcined at various temperatures.

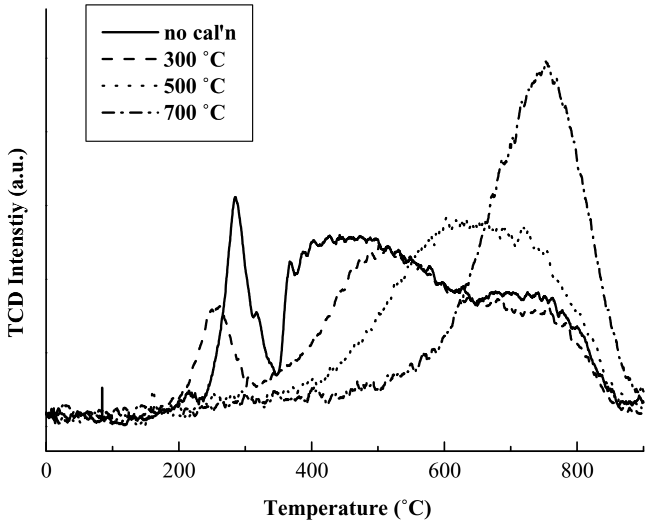

Fig. 3. The TPR spectra of NiO/$M_{2.2}T$ calcined at various temperatures.

The peak area for Ni reduction on $M_{2.2}T$ changed insignificantly with increasing calcination temperatures while that for the Ni reduction on MgO decreased dramatically. We believe this difference was originated from whether solid solution formed or not, which was discussed in the next section.

Table 4 summarized the TPR results for all of the prepared samples. Peaks were deconvoluted and maximum peak positions and relative peak areas were provided for comparison. Small peaks with areas less than 5% of total peak area were ignored. Reduction peaks of the highest temperatures for all samples shifted to higher temperatures as calcinations temperatures were increased. For the first four samples, TiO_2, $M_{0.6}T$, M_1T and $M_{1.5}T$, the Ni reduction peaks of their highest temperatures appeared below 700 °C. On the contrary, for the next five samples having relatively higher Mg fraction in the support materials, $M_{2.2}T$–M_8T, the reduction peaks appeared above 740 °C as the calcination temperatures were increased. In order to find out the relationship between reduction patterns and oxidation states of nickel, XRD analyses were performed.

3.5. X-ray diffraction (XRD)

The crystalline phases of the Ni/MgO–TiO_2 composite oxides having various Mg to Ti molar ratios were identified by X-ray diffraction. Fig. 4 indicated crystalline phases of each sample calcined at 700 °C. Several phases could exist due to co-existence of three different metal components, which include karooite ($MgTi_2O_5$), geikielite ($MgTiO_3$), qandilite (Mg_2TiO_4), nickel titania ($NiTiO_3$) and the solid solution of $Ni_xMg_{1-x}O$. Unfortunately, however, many XRD peaks of these phases overlap each other so that it is almost impossible to identify the existing phases without ambiguity. The assigned peaks are as follows: (a) 29.90° for Mg_2TiO_4 (2 2 0), (b) ∼35° for $NiTiO_3$ (1 0 4) and for $MgTiO_3$ (1 0 4), and (c) ∼43° for NiO (0 0 3) and MgO (1 1 1), respectively.

Table 4
Results of deconvoluted TPR curves of various catalysts calcined at different temperatures

Calcination temperature(°C)	TiO_2		$M_{0.6}T$		M_1T		$M_{1.5}T$		$M_{2.2}T$	
	Peak[a]	Ratio	Peak	Ratio	Peak	Ratio	Peak	Ratio	Peak	Ratio
300	320	0.69	392	0.73	401	0.38	403	0.48	255	0.11
	402	0.29	516	0.27	504	0.62	532	0.52	520	0.65
									739	0.25
500	386	0.65	397	0.57	439	0.23	446	0.36	313	0.07
	469	0.35	512	0.43	539	0.77	577	0.64	619	0.77
									762	0.16
700	589	0.92	420	0.53	468	0.36	481	0.31	740	1.00
	641	0.09	690	0.47	668	0.64	696	0.69		
	M_3T		M_5T		M_7T		M_8T		MgO	
	Peak	Ratio	Peak	Ratio	Peak	Ratio	Peak	Ratio	Peak	Ratio
300	235	0.07	490	0.39	550	0.60	553	0.51	690	1.00
	439	0.29	726	0.59	782	0.38	760	0.43		
	545	0.06								
	676	0.59								
500	591	0.39	590	0.34	360	0.09	331	0.08	734	0.96
	638	0.57	661	0.48	648	0.56	691	0.84		
				0.18	823	0.35	845	0.08		
700	765	1.00	535	0.27	471	0.21	490	0.23	398	0.12
			798	0.73	819	0.56	790	0.77	949	0.88

[a] Maximum temperature of peak (°C).

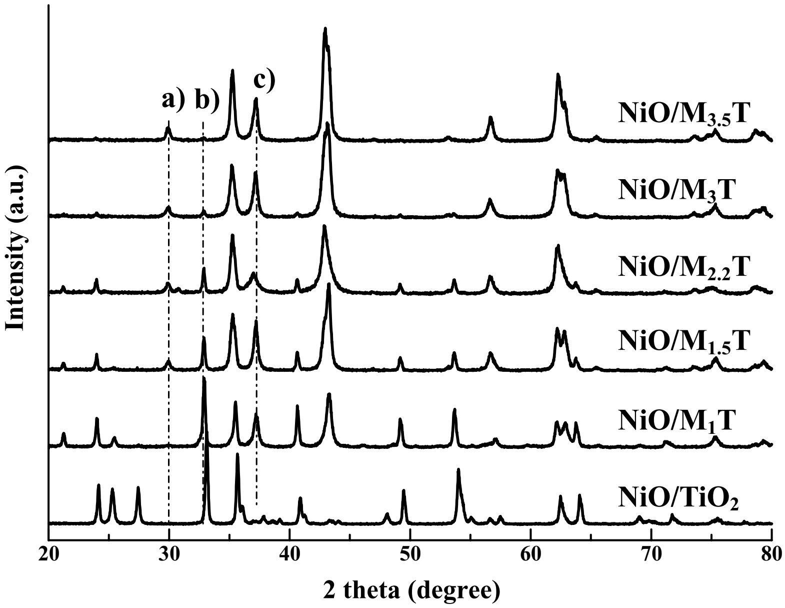

Fig. 4. XRD patterns of nickel oxide supported on various supports with different ratios of Mg to Ti calcined at 700 °C: (a) Mg_2TiO_4 (2 2 0), (b) $MgTiO_3$ (1 0 4) and $NiTiO_3$ (1 0 4), and (c) NiO (0 0 3) and MgO (1 1 1). Catalyst code can be different from actual crystalline phase.

The peak pattern in very bottom of Fig. 4 was of the sample noted as NiO/TiO_2, but turned out to be $NiTiO_3$. No NiO peak was found. The support of M_1T consisted of single phase $MgTiO_3$. The composite oxide samples having the molar ratio of 1.5 or larger turned out to have Mg_2TiO_4 phase. The samples of $NiO/M_{1.5}T$ and $NiO/M_{2.2}T$ also have $MgTiO_3$, Mg_2TiO_4, NiO, and MgO phases. While the geikielite ($MgTiO_3$) disappeared for the oxide samples having Mg to Ti ratio of 3 or larger, the qandilite (Mg_2TiO_4) remained in the samples with the ratios beyond 7 (not shown).

Fig. 5 is enlarged image of the XRD patterns of the Ni samples on calcined magnesium rich oxides (M_3T, M_5T, M_7T, and M_8T) and on MgO between 42 and 44°. In this region, three peaks can be assigned to Mg_2TiO_4 (4 0 0) at 42.82°, MgO (2 0 0) at 43.04°, and NiO (0 1 2) at 43.29°, respectively. The peak pattern of NiO was not at its original positions, but shifted to smaller 2 theta. For the Ni supported on M_xT, there was no peak shift regardless of the composition of the supports. In contrast, the peak of NiO/MgO shifted to larger angle, which clearly indicates formation of solid solution.

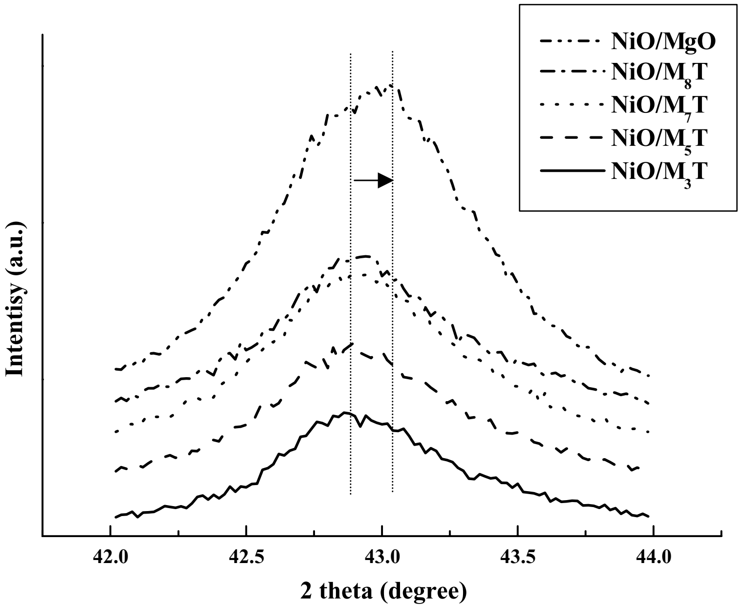

Fig. 5. Enlarged XRD peaks of supported nickel oxides on various supports.

4. Discussion

4.1. Activity and resistance to the deactivation of catalyst

Considering the catalytic activities obtained before and after Li poisoning in Table 2, the prepared catalysts can be put into three categories. These are Ti-rich catalysts (Ni/TiO_2, Ni/$M_{0.6}T$, Ni/M_1T), Mg-rich catalysts (Ni/MgO and Ni/M_8T), and intermediate catalysts ($M_{2.2}T$–M_7T). The Ti-rich and the Mg-rich catalysts lost almost all of their activities after Li poisoning; however, the intermediate catalysts maintained their activities more than a half of their original activities even after Li poisoning. This is somewhat consistent with our previous report [18] where qandilite (Mg_2TiO_4) kept more activity than karooite ($MgTi_2O_5$) and geikielite ($MgTiO_3$) after Li poisoning.

Comparing Table 2 with Table 3, decrease in BET surface area seemed not to be a major reason for activity loss. Although the Li poisoning caused dramatic decrease in the BET surface area, some of the catalysts, especially the intermediate catalysts, sustained their activities with less amounts. This implies that the blocking of pore structure and/or the collapse of support structure are not major causes of deactivation, which is similar to the results described in other reports [4,7]. Instead, avoiding formation of mixed oxide and/or solid solution between Ni and support materials turned out to be more important in reducing Li poisoning as discussed below with XRD data.

4.2. Effect of TiO_2 addition to Ni/MgO catalyst on reforming catalytic activity

The Ni–MgO and Ni–TiO_2 interactions for supported Ni on each metal oxide support have been widely studied [11,12,15,17,24–26]. No report could be found, however, concerning the Ni interaction with composite oxide of MgO–TiO_2 since this composite oxide has never been used as a support material to our best knowledge.

Experimental results of TPR for the NiO/TiO_2 sample calcined at different temperatures were shown in Fig. 1. Three reduction peaks approximately at 320, 390 and 590 °C were assigned to the unsupported NiO, strong interacted NiO, and $NiTiO_3$, respectively [24,26]. The sample calcined at 500 °C seemed to have maximum NiO–support interaction among the calcined samples employed since it showed the NiO reduction peak at the highest temperature without forming nickel titanate ($NiTiO_3$). The sample calcined at 700 °C also showed reduction peaks, but transformed confirmatively to nickel titanate, as shown in Fig. 4. Even though calcination step is usually required to prepare well-dispersed metal oxide catalysts on a support, calcining NiO/TiO_2 sample at 700 °C resulted in unwanted phase transition of the catalyst.

For the Ti-rich catalysts, the maximum reduction temperatures did not exceed 700 °C, similar to the TPR result for the nickel Ni/TiO_2 sample. This similarity in reduction temperature indicates that adding as much as equal fraction of MgO to TiO_2 support to make composite oxide support did not affect the Ni–support interaction significantly. The existence of $NiTiO_3$ phase for the Ti-rich catalysts could not be identified due to overlapping in the XRD patterns between $NiTiO_3$ and $MgTiO_3$. Hence, it is not possible to determine at this moment whether the strong Ni–support interaction deduced from high reduction peak is originated from the formation of $NiTiO_3$. However it is clear that the incorporated Mg into the TiO_2 support changed insignificantly the Ni–support interaction, considering the results shown in Fig. 2. If the introduced Mg affected Ni–support interaction, the Ni reduction temperature should have shifted to higher temperatures, as discussed below.

As shown in Fig. 2, calcining the NiO–MgO at more than 700 °C resulted in shift of starting reduction temperature to higher temperature and in decrease of total reduction area. This is believed to be owing to the formation of irreducible $Ni_xMg_{1-x}O$ solid solution as discussed by Arena et al. [27]. According to Antolini [14], the dissolving rate of nickel ion into MgO matrix can be accelerated by the assistant lithium, which formed $Li_yNi_xMg_{1-y-x}O$. We believed that no activity of the NiO/MgO sample after Li poisoning in our study must be a consequence of this $Li_yNi_xMg_{1-y-x}O$ formation; irreducible nickel cannot catalyze the methane reforming reaction.

The samples having relatively small fraction of Ti (M_5T, M_7T, and M_8T) showed distinguishable characteristics from the NiO/MgO system regarding the TPR results (Table 4). For the samples calcined at 700 °C, known to be a sufficient temperature to form solid solution for the NiO/MgO oxide, the reduction peaks appeared at ∼800 °C. If the solid solution were formed, not only the reduction peak would have shifted to higher temperatures, but also the peak area would have decreased.

Consequently, adding small fraction of Ti to the NiO/MgO system turned out to be effective in obstructing $Ni_xMg_{1-x}O$ solid solution. This result can be confirmed by the XRD results. Since Arena's work [27], the peak shift in X-ray diffraction became accepted as a reasonable method to distinguish whether a solid solution formed or not. As shown in Fig. 5, the diffraction patterns for the Mg-rich catalysts placed almost at the same angle even though the composition of the material was changed. This observation strongly suggests that relatively small fraction of Ti hindered the formation of $Ni_xMg_{1-x}O$ solid solution as proved additionally in the TPR results and strengthened the structure of the Mg-rich catalysts so that the effect of Li poisoning on catalytic activity weakened.

5. Conclusions

Effects of TiO_2 addition to the MgO support in NiO/MgO methane reforming catalysts system for DIR-MCFC on their activities and resistances to Li poisoning, were investigated. When Li_2CO_3 was not introduced to the reforming catalysts, the NiO/MgO–TiO_2 catalysts turned out to be active regardless of Mg/Ti ratio. However, when Li_2CO_3 was introduced to the reforming catalysts, all of the NiO/MgO–TiO_2 catalysts were poisoned and revealed decreased activities with different degrees. The NiO/MgO–TiO_2 catalysts with the Mg/Ti ratios of 2–7 sustained approximately 60% of their original activities. The results obtained by the temperature-programmed reduction and the X-ray diffraction suggested that addition of relatively small fraction of TiO_2 into the NiO/MgO reforming catalyst system resulted in obstructing the formation of $Ni_xMg_{1-x}O$ solid solution and increasing resistance to Li poisoning.

Acknowledgements

This work was financially supported by Korea Electric Power Research Institute through Korea Institute of Science and Technology, and by Korea Science and Engineering Foundation through Research Center for Energy Conversion and Storage.

References

[1] R.J. Selman, Energy 11 (1986) 153.
[2] S. Cavallaro, S. Freni, R. Cannistraci, M. Aquino, N. Giordano, Int. J. Hydrogen Energy 17 (1992) 181.
[3] R.J. Rostrup-Nielsen, L.J. Christiansen, Appl. Catal. A: Gen. 126 (1995) 381.
[4] R.J. Berger, E.B.M. Doesburg, J.G. van Ommen, J.R.H. Ross, Appl. Catal. A: Gen. 143 (1996) 343.
[5] R.J. Berger, E.B.M. Doesburg, J.G. van Ommen, J.R.H. Ross, J. Electrochem. Soc. 143 (1996) 3186.
[6] M. Matsumura, C. Hirai, Ind. Eng. Chem. Res. 37 (1998) 1793.
[7] M. Matsumura, C. Hirai, J. Chem. Eng. Jpn. 31 (1998) 734.
[8] H.-D. Moon, T.-H. Lim, H.-I. Lee, Bull. Korean Chem. Soc. 20 (1999) 1413.
[9] H.-D. Moon, J.-H. Kim, H.Y. Ha, T.-H. Lim, S.-A. Hong, H.-I. Lee, J. Korean Ind. Eng. Chem. 10 (1999) 754.
[10] H.-D. Moon, Ph.D. Thesis, Seoul National University, Seoul, Korea, 1999.
[11] F. Arena, F. Frusteri, A. Parmaliana, Appl. Catal. A: Gen. 187 (1999) 127.
[12] F. Arena, F. Frusteri, L. Plyasova, A. Parmaliana, J. Chem. Soc., Faraday Trans. 94 (1998) 3385.
[13] F. Arena, A.L. Chuvilin, A. Parmaliana, J. Phys. Chem. 99 (1995) 990.
[14] E. Antolini, Mater. Lett. 51 (2001) 385.
[15] E. Ruckenstein, Y.H. Hu, Appl. Catal. A: Gen. 183 (1999) 85.
[16] A. Parmaliana, F. Arena, F. Frusteri, S. Coluccia, L. Marchese, G. Martra, A.L. Chuvilin, J. Catal. 141 (1993) 34.
[17] J. van de Loosdrecht, A.M. van der Kraan, A.J. van Dillen, J.W. Geus, J. Catal. 170 (1997) 217.
[18] J.-S. Choi, J.-S. Choi, T.-H. Lim, H.-I. Lee, in: Proceedings of the Eighth Japan–Korea Symposium on Catalysis, Young Scientist Session, 2001, p. 53.
[19] K. Tanabe, H. Hattori, T. Sumiyoshi, K. Tamaru, T. Kondo, J. Catal. 53 (1978) 1.
[20] T. Lopez, J. Hernandez, R. Gomez, X. Bokhimi, J.L. Boldu, E. Munoz, O. Novaro, A. Garcia-Ruiz, Langmuir 15 (1999) 5689.
[21] X. Bokhimi, J.L. Boldu, E. Munoz, O. Novaro, T. Lopez, J. Hernandez, R. Gomez, A. Garcia-Ruiz, Chem. Mater. 11 (1999) 2716.
[22] K.S. Jung, B.-Y. Coh, H.-I. Lee, Bull. Korean Chem. Soc. 20 (1999) 89.
[23] Y.J. Shin, H.-D. Moon, T.-H. Lim, H.-I. Lee, Stud. Surf. Sci. Catal. 130 (2000) 431.
[24] Q.G. Yan, W.Z. Weng, H.L. Wan, H. Toghiani, R.K. Toghiani, C.U. Pittman Jr., Appl. Catal. A: Gen. 239 (2003) 43.
[25] M.C.J. Bradford, M.A. Vannice, Catal. Today 50 (1999) 87.
[26] P.S. Kumbhar, Appl. Catal. 96 (1993) 241.
[27] F. Arena, F. Frustrei, A. Parmaliana, L. Plyasova, A.N. Shmakov, J. Chem. Soc., Faraday Trans. 92 (1996) 469.